Design of a Unidirectional Laser by using a Nd-doped Al_2O_3 Taiji Resonator for Sensing Purposes

D. J. M. Wojcik, C. E. Osornio-Martínez, B. Jongebloed, and S. M. García-Blanco

Integrated Optical Systems, MESA+ Institute for Nanotechnology, University of Twente, 7500 AE Enschede, The Netherlands

In the health and medicine fields, continuously higher demands are set for the sensitivity and limit of detection (LOD) of sensors. Photonic Integrated Circuits (PICs) have the potential to achieve high performance. However, many sensors are being made with passive material, which leaves a lot of room to improve the LOD. In this work, a design of an active Nd^{3+}: Al_2O_3 Taiji resonator is proposed. The design has the potential for both exceptional point sensing and unidirectional lasing. The power coupling of the coupling sections is optimised for a pump wavelength of 800 nm and a lasing wavelength of 1064 nm.

Introduction

In the health and medicine fields, biosensors are necessary to detect diseases, concentrations of solvents, or dangerous pollutants. Photonic Integrated Circuits (PICs) have a potential to improve the sensitivity and limit of detection of such sensors. However, they must be low-cost, easy to use, small, fast and accurate. Sensing on PICs can be done by immobilizing a layer of capture probes on the surface of a waveguide, so that biomarker molecules can be attached to the surface. The presence of these molecules then changes the effective refractive index of the waveguide, which translates to a change of optical path length that is detected by the sensor.

By using active resonators, the linewidth can be reduced [1] and it is expected that this will reduce the LOD. In previous work of the research group, ytterbium has been used for a laser at 1 μm [2]. However, the slope efficiency of the laser is low (~0.1%) and the laser threshold is high because the ytterbium has a simple two-level energy scheme. In this work, neodymium will be used to dope the Al_2O_3 core material. Neodymium has a four-level system, with emission wavelength 1.06 μm. A four-level gain medium does not have the problem of reabsorption of the lasing wavelength, while two- or three-level gain media do.

In this work, an active Taiji resonator (i.e., a Taiji laser) design is proposed. A Taiji resonator is a microring resonator (MRR) with an additional S-waveguide in the middle of the resonator cavity, as shown in Figure 1 [3]. This design permits a further increase of the sensitivity by working at the exceptional point [4]. At this point, the sensitivity exceeds the sensitivity that can be obtained in Hermitian systems.

Moreover, Taiji lasers have been shown to robustly lase unidirectionally [5, 6], since the clockwise (CW) mode in the ring can couple to the counterclockwise (CCW) mode, but not the other way around. Furthermore, the design of a Taiji laser has been theoretically investigated [7]. The results of this research will serve as the basis for design choices for the optimal coupling lengths of the S-waveguide.

The combination of Al_2O_3 and Nd is novel, since so far, only one device has been made with the end goal of making an optical backplane [8]. There, amorphous Nd^{3+}: Al_2O_3 was used to create amplifiers at wavelengths of 880 nm, 1064 nm and 1330 nm. The maximum gain that was achieved for 1064 nm was 6.3 dB/cm.

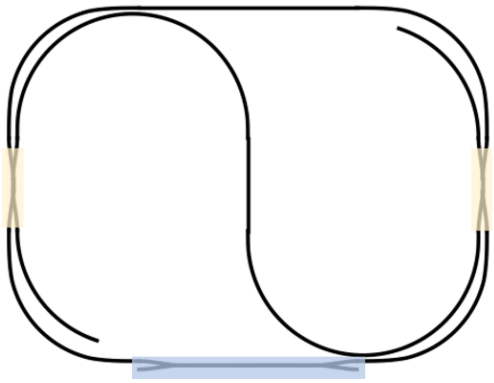

Figure 1: Schematic overview of the design of the Taiji resonator. The yellow areas indicate the S-waveguide coupling sections and the blue area indicates the coupling section with the bus waveguide. The ends of the S-waveguide are tapered and are terminated at an angle to prevent back reflections.

Methods and Materials

RF reactive magnetro co-sputtering (AJA ATC 1500) is used to deposit an $Nd^{3+}:Al_2O_3$ layer on a SiO_2 wafer with a controlled oxygen flow. The loss of a $Nd^{3+}:Al_2O_3$ slab waveguide without cladding was measured with a prism coupling setup (Metricon 2010/M) and the results are shown in Figure 2. At 521 nm, there is higher loss, due to an absorption peak of neodymium at this wavelength.

Poly-crystalline aluminium oxide will be used as the core material of the waveguides. As a laser sensor base, this material has many advantages such as its broad transparency range, its high solubility for rare-earth ions, and its high refractive index, which enables compact PIC design.

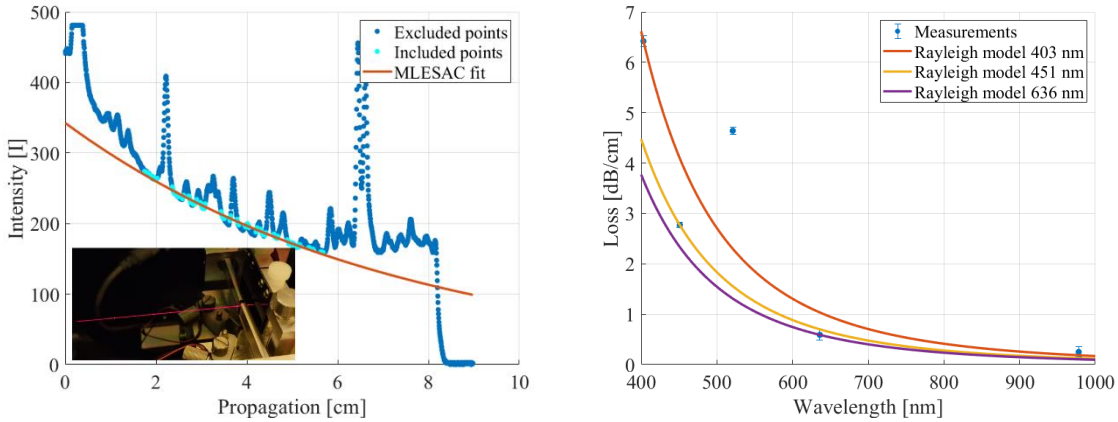

Figure 2: (a) The propagation of a $Nd^{3+}:Al_2O_3$ slab waveguide for a wavelength of 636 nm with a loss of 0.58 ± 0.12 dB/cm. Including a picture of the 636 nm guiding mode in the experimental prism coupling set up. (b) Propagation loss plotted as a function of wavelength. The loss at 521 nm is high, due to an absorption peak of Nd. Dots represent measured losses while the lines are fits based on a Rayleigh scattering model.

Simulations and designs

For the design of the Taiji laser, several parameters must be simulated and optimised to achieve performance near optimal conditions. First, the modal field in the waveguides must be analysed and the dimensions must be chosen. A schematic overview of the waveguide cross section and materials is shown in Figure 3. For the cladding material, PMMA is used, which was shown to exhibit low propagation losses at the wavelength range of interest (i.e., around 1 μm).

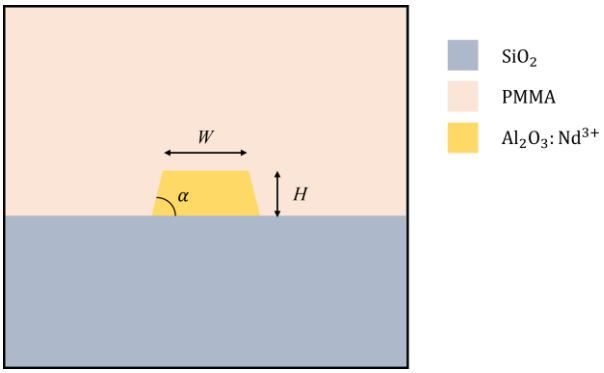

Figure 3: A schematic view of the waveguide cross section, with W as the width, H as the thickness and α as the wall angle of the waveguide.

The waveguide cross section was simulated using Lumerical Mode Solutions software and three widths for the designs are chosen such that there is one monomode waveguide, one bimodal waveguide and one geometry which is on the edge having one and two modes. The widths are 1 µm, 1.6 µm and 1.3 µm, respectively. In principle, it is desirable to have a monomodal waveguide. However, a higher confinement of the mode is obtained as the waveguide dimensions increase. This leads to a higher overlap of the pump field with the gain material, which in turn results in a higher gain. The confinement of the pump field for the smallest cross section is 72.9% and for the largest cross section 78.1%. The thickness of the fabricated slab waveguide was used for the simulations, which was 376 nm.

The coupling section with the bus waveguide must be optimised such that the coupling power is minimised for the signal wavelength and is maximised for the pump wavelength. The optimisation is done by using supermode theory. The effective refractive index is simulated with the Finite-Difference Eigenmode solver for the odd and even modes in the coupling section. These effective refractive indices are then used to calculate the coupling coefficients of the coupling sections, using equations from [9]. The resulting simulation is shown in Figure 4a. In this figure, the power coupling is plotted as a function of coupling length for the pump and signal wavelength. Additionally, the optimal coupling length is indicated with a dashed and dotted vertical line. The gap width between the two waveguides was set to 0.6 µm.

The same principle is used to determine the optimal coupling for the S-waveguide couplers. However, in this case, the amount of coupling for the signal wavelength is restricted to the following rules of thumb: $\sqrt{\gamma_S/\gamma_A} \geq 0.5$ and $\gamma_S/\gamma_A \leq 1$ [7]. Where γ_A is the intrinsic loss of the ring and γ_S is the loss due to the coupling with the S-waveguide. The first rule of thumb is the minimal restriction for having robust unidirectional lasing, such that there is no spontaneous switching between the CW and CCW modes. The second rule of thumb is the upper limit for the coupling to the S-waveguide, such that the laser threshold is not too high.

γ_A is estimated by using the loss measurements of similar designs in the group, which is 26.4 dB/m [4]. In Figure 4b, the power coupling is plotted. Moreover, the maximum and minimum coupling lengths are indicated with vertical lines. For these coupling sections, a larger gap width of 1.2 µm was chosen to make the lengths long enough for fabrication.

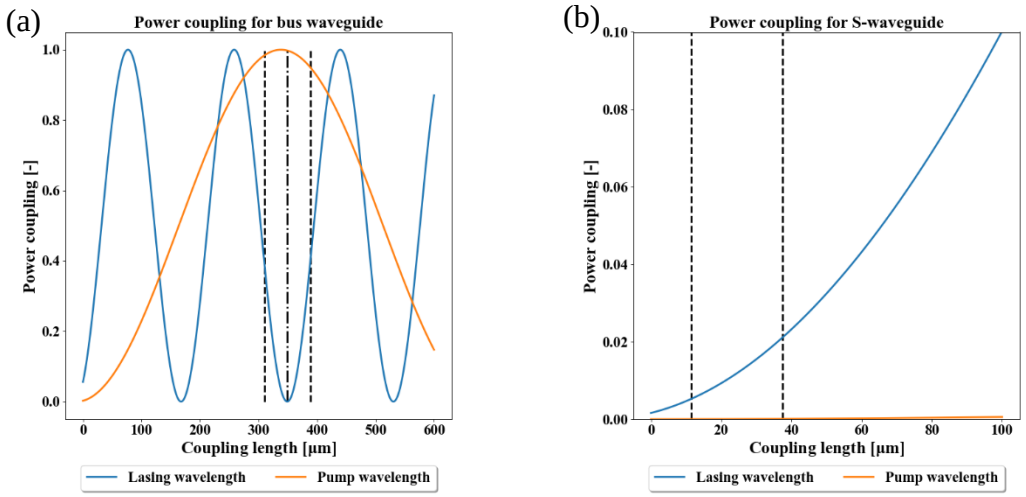

Figure 4: Power coupling simulation results for the coupling sections of the bus waveguide (a) and S-waveguide (b). Upper and lower limits of the optimal coupling are indicated with dashed lines. The width of the waveguides is 1 µm and the gap width used for (a) is 0.6 µm and for (b) is 1.2 µm.

Conclusion

The coupling sections of the Taiji laser were investigated by simulations. Ultimately, the optimal coupling lengths for lasing at 1.06 µm are 348.9 µm for the coupling to the bus waveguide and the coupling for the S-waveguide should be between 11.4 µm and 37.4 µm. The coupling lengths of all coupling sections should be varied around the simulated values, such that fabrication variations can be taken into account.
The next step in the project is to fabricate the design with E-beam lithography for multiple concentrations of neodymium doping. Afterwards, the devices will be characterised and further optimization will be carried on.

References

[1] L. He, S. ¸ Ahin, K. Ozdemir, and L. Yang, "Whispering gallery microcavity lasers," 2012, doi: 10.1002/lpor.201100032.

[2] M. de Goede *et al.*, "Al2O3:Yb3+ integrated microdisk laser label-free biosensor," 2019, doi: 10.1364/OL.44.005937.

[3] L. Pavesi *et al.*, "Unidirectional reflection from an integrated 'taiji' microresonator," *Photonics Research, Vol. 8, Issue 8, pp. 1333-1341*, vol. 8, no. 8, pp. 1333–1341, Aug. 2020, doi: 10.1364/PRJ.393070.

[4] B. Jongebloed, "Integrated Optical Self-Referenced Sensing at the Exceptional Point," University of Twente, Enschede, 2022.

[5] J. P. Hohimer and G. A. Vawter, "Unidirectional semiconductor ring lasers with racetrack cavities," *Appl. Phys. Lett*, vol. 63, p. 2459, 1993, doi: 10.1063/1.110474.

[6] S. Kharitonov and C. S. Brès, "Isolator-free unidirectional thulium-doped fiber laser," *Light: Science & Applications 2015 4:10*, vol. 4, no. 10, pp. e340–e340, Oct. 2015, doi: 10.1038/lsa.2015.113.

[7] A. Muñoz de las Heras and I. Carusotto, "Unidirectional lasing in nonlinear Taiji microring resonators," *Phys Rev A (Coll Park)*, vol. 104, no. 4, p. 043501, Oct. 2021, doi: https://doi.org/10.1103/PhysRevA.104.043501.

[8] J. Yang, "Neodymium-doped Waveguide Amplifiers and Lasers for Integrated Optical Applications," University of Twente, Enschede, 2010.

[9] M. Bahadori *et al.*, "Design Space Exploration of Microring Resonators in Silicon Photonic Interconnects: Impact of the Ring Curvature," *Journal of Lightwave Technology*, vol. 36, no. 13, pp. 2767–2782, Jul. 2018, doi: 10.1109/JLT.2018.2821359.